Influence of the scan timepoint when assessing hypoxia in ^{18}F-fluoromisonidazole PET: Two versus four hours

Kentaro Kobayashi, MD, PhD[1], Osamu Manabe, MD, PhD[1], Kenji Hirata, MD, PhD[1,*], Shigeru Yamaguchi, MD, PhD[2], Hiroyuki Kobayashi, MD, PhD[3], Shunsuke Terasaka, MD, PhD[3], Takuya Toyonaga, MD, PhD[4], Sho Furuya, MD[1], Keiichi Magota, PhD[5], Yuji Kuge, PhD[6], Kohsuke Kudo, MD, PhD[7,8], Tohru Shiga, MD, PhD[1], Nagara Tamaki, MD, PhD[9]

Drs. Kobayashi and Manabe contributed equally to this study.

[1]Department of Diagnostic and Interventional Radiology, Hokkaido University Hospital, Sapporo, Japan

[2]Department of Neurosurgery, Hokkaido University Graduate School of Medicine, Sapporo, Japan

[3]Kashiwaba Neurosurgery Hospital, Sapporo, Japan

[4]PET Center, Department of Radiology and Biomedical Imaging, Yale University School of Medicine, New Haven, Connecticut, USA

[5]Division of Medical Imaging and Technology, Hokkaido University Hospital, Sapporo, Japan

[6]Central Institute of Isotope Science, Hokkaido University, Sapporo, Japan

[7]Department of Diagnostic Imaging, Hokkaido University Graduate School of Medicine, Sapporo, Japan

[8]Global Station for Quantum Medical Science and Engineering, Global Institution for Collaborative Research and Education, Hokkaido University

[9]Department of Radiology, Kyoto Prefectural University, Kyoto, Japan

***Corresponding author:** Dr. Kenji Hirata, Department of Diagnostic and Interventional Radiology, Hokkaido University Hospital, Kita 15, Nishi 7, Kita-Ku, Sapporo, Hokkaido 060-8638, Japan. Tel.: +81-11-706-7779; Fax.: +81-11-706-7408

Email: khirata@med.hokudai.ac.jp

Total word count: 5705

Running title: Optimizing scan timing in FMISO PET

ABSTRACT

Purpose: ^{18}F-fluoromisonidazole (^{18}F-FMISO) is the most widely used positron emission tomography (PET) tracer for imaging tumor hypoxia. Previous reports suggested that the time from injection to the scan may affect the assessment of ^{18}F-FMISO uptake. Herein we directly compared the images at 2 hr and 4 hr after a single injection of ^{18}F-FMISO.

Methods: Twenty-three patients with or suspected of having a brain tumor were scanned twice at 2 and 4 hr following an intravenous injection of ^{18}F-FMISO. We estimated the mean standardized uptake value (SUV) of the gray matter and white matter and the gray-to-white matter ratio in the background brain tissue from the two scans. We also performed a semiquantitative analysis using the SUVmax and maximum tumor-to-normal ratio (TNR) for the tumor.

Results: At 2 hr, the SUVmean of gray matter was significantly higher than that of white matter (median 1.23, interquartile range (IQR) 1.10–1.32 *vs.* 1.04, IQR 0.95–1.16, $p<0.0001$), whereas at 4 hr, it significantly decreased to approach that of the white matter (1.10, IQR 1.00–1.23 *vs.* 1.02, IQR 0.93–1.13, p=NS). The gray-to-white matter ratio thus significantly declined from 1.17 (IQR 1.14–1.19) to 1.09 (IQR 1.07–1.10) ($p<0.0001$). All 7 patients with glioblastoma showed significant increases in the

SUVmax (2.20, IQR 1.67–3.32 at 2 hr *vs.* 2.65, IQR 1.74–4.41 at 4 hr, p=0.016) and the TNR (1.75, IQR 1.40–2.38 at 2 hr *vs.* 2.34, IQR 1.67–3.60 at 4 hr, p=0.016).

Conclusion: In the assessment of hypoxic tumors, ^{18}F-FMISO PET for hypoxia imaging should be obtained at 4 hr rather than 2 hr after the injection.

Keywords: fluoromisonidazole, positron emission tomography, glioblastoma, hypoxia, scan timing

Introduction

Hypoxia, i.e., lack of oxygen, causes poor prognoses in patients with malignant tumors [1-3]. Clinically, there is strong evidence that the poor prognoses are due to the effects of hypoxia on therapy resistance and malignant progression [4]. ^{18}F-fluoromisonidazole (^{18}F-FMISO) positron emission tomography (PET) is a promising and noninvasive method for *in vivo* hypoxia imaging [5-8]. Valk et al. first evaluated the ^{18}F-FMISO uptake in glioma in 1992 [9], and subsequent reports demonstrated the usefulness of ^{18}F-FMISO for the assessment of glioma differentiation and prognosis [8, 10-18].

Glioblastoma (GBM), which is classified among gliomas as World Health Organization (WHO) grade IV [19, 20], is the most malignant glioma, requiring multidisciplinary treatment. Histopathologically, GBM is characterized by the presence of palisading necrosis and hyperplastic blood vessels. We have demonstrated that ^{18}F-FMISO PET has the potential to distinguish GBM from lower-grade gliomas [21]. We also observed a strong relationship between the presence of necrosis and ^{18}F-FMISO uptake, regardless of the pathological subtype [22]. However, other studies have reported that ^{18}F-FMISO uptake was observed in not only GBMs but also lower-grade gliomas [12, 17, 23]. This discrepancy might be due to the difference in the scan

timepoint following ^{18}F-FMISO administration. The scan time used in literature for imaging hypoxia in brain tumors is variable, ranging from 120 min (or even less in some papers) to 240 min post-injection. The lack of standardization has led to inconsistency of data. Therefore, there is a need to establish the precise scanning time which most accurately reflects hypoxia. Both 2-hr and 4-hr scanning protocols have advantages and disadvantages. In the present retrospective analysis, we focused on the ability of ^{18}F-FMISO PET to discriminate between GBM and non-GBM at 2 hr and 4 hr after a single injection of ^{18}F-FMISO, and directly compared the images taken at the two scanning time points to determine their ability to visualize hypoxia.

Materials and Methods

Study subjects

The Ethics Committee of Hokkaido University Hospital approved this retrospective study (IRB No. 015-0159). We analyzed the cases of the patients who had brain parenchymal tumor-like lesions with a maximum diameter of ≥2 cm on magnetic resonance (MR) imaging from September 2014 to July 2015 at our hospital. This study included both patients who were at initial diagnosis and those being evaluated for lesion recurrence. Only patients who could undergo two PET scans at 2 hr and 4 hr after an

injection of ^{18}F-FMISO were included in this study.

Image acquisition and reconstruction

For each patient, ^{18}F-FMISO was injected once, and PET images were acquired twice at 2 and 4 hr after the injection (Fig. 1). All clinical PET images were acquired using a single scanner (Gemini GXL 16 PET/CT; Hitachi Medical, Tokyo). The injected dosage of ^{18}F-FMISO was 395.0 (interquartile range [IQR] 388.0–410.0) MBq. The duration of each emission scan was 20 min. X-ray CT scanning was performed before the emission scanning for attenuation correction. The images were reconstructed by a line of response-row action maximum-likelihood algorithms with the following settings: number of iterations, 2; relaxation parameter, 0.2813; blob radius, 3.234 pixels; alpha, 9.5088; increment, 2.0375. The image matrix size was 128 * 128 pixels for the 256-mm field of view (FOV), and the voxel size was 2 mm^3. The reconstructed images were not additionally post-filtered.

Image analysis

The PET images were three-dimensionally coregistered to T1-weighted MR images before and after the contrast medium injection with the use of the SPM8

software package [10]. An experienced nuclear medicine physician (K.K.) visually validated that there was no mis-coregistration. The ^{18}F-FMISO radioactivity concentrations in the background brain tissues and in the lesions were then evaluated both visually and semi-quantitatively. For the visual analysis, two readers who were experienced in nuclear medicine (K.K. and O.M.), and who were masked to the patients' clinical information, imaging reports, and the other reader's interpretation, independently reviewed the ^{18}F-FMISO PET/CT images. A third experienced reader (K.H.) who was also masked to the clinical information and image interpretations was included to resolve any differences in interpretation by the two primary readers, by consensus review. The information as to whether the patients had undergone treatments before the PET scan was also masked, but the readers could guess it from MRI data. A difference in pattern definition among the three observers was settled by consensus. For the semi-quantitative analysis, an experienced nuclear medicine physician (K.K.) placed regions of interest (ROIs) in each lesion by referring to the MR images, while blinded to the pathological diagnosis.

The gray-to-white matter contrast (GWC) in the background brain tissue was evaluated first. The GWC was defined as positive when the uptake in the gray matter was higher than that in the white matter. The GWC was defined as negative when the

uptake in the gray matter was equal to that in the white matter (Fig. 2). In the semi-quantitative assessment, the radioactivity concentrations in the background brain tissues were obtained as follows: circular 10-mm-diameter ROIs were placed on the cerebral gray matter, the cerebral white matter, and the cerebellar cortex. A total of 30 ROIs (5 per side × 2 sides per slice × 3 slices) were placed on each region [21]. The standardized uptake values (SUVs) were calculated from all of the voxels within these ROIs. The SUV was defined as [tissue radioactivity concentration (Bq/ml)] × [body weight (g)]/[injected radioactivity (Bq)].

For the assessment of the tumor lesions, the ^{18}F-FMISO uptakes were visually categorized into two groups. The uptake was considered positive when the lesion uptake was higher, and negative when the lesion uptake was equal to or lower than that of the surrounding brain tissues (Fig. 2).

For an additional assessment, 12 patients with histologically confirmed glioma were evaluated visually and quantitatively to compare the grade IV gliomas (i.e., the GBMs) with the gliomas that were ≤grade III (the non-GBMs). For the quantitative assessment of the tumor lesions, we calculated the maximum SUV (SUVmax) and the tumor-to-normal ratio (TNR) as in the previous study [21]. Minimum and mean SUV were not used because they are easily affected by the ROI size and position. The

SUVmax was the SUV of the voxel having the highest SUV in the entire lesion. The TNR was defined as the SUVmax divided by the reference value, which was derived from the cerebellar ROIs [10].

Surgical procedures

The detailed procedures of our subjects' PET-guided surgeries were described previously [24]. In brief, all surgical operations were performed under a neuro-navigation system (StealthStation™ Treon® or S7®; Medtronic, Minneapolis, MN). Before each surgery, the ^{18}F-FMISO uptake lesions were superimposed onto MR T1-weighted images with gadolinium enhancement. When a patient underwent a biopsy, the biopsy target was set in the ^{18}F-FMISO uptake lesion under the navigation system if the ^{18}F-FMISO uptake lesion was identified. When a patient underwent a maximum tumor resection, the ^{18}F-FMISO accumulation areas were contained in the area of the resection as much as possible.

Each pathological diagnosis was determined by agreement between the two experienced neuropathologists based on the 2007 WHO classification [19, 20].

Statistical analyses

All parametric variables are presented as medians with the IQR. Categorical variables are presented as absolute numbers with percentages. A p-value of <0.05 was considered significant. The Wilcoxon signed-rank test was used for inter-group comparisons. Fisher's exact test was used to compare discrete data. The diagnostic performances of TNR and the identification of the optimal cutoff points for the differentiation between GBM and non-GBM were evaluated using receiver operating characteristic (ROC) curves and the assessment of the area under the ROC curve (AUC). Statistical calculations were carried out using JMP Pro ver. 14 software (SAS, Cary, NC).

Results

Patients

The cases of 23 patients were retrospectively analyzed: 10 males, 13 females; age 61 yrs (IQR 47–68 yrs) (Table 1). The first and second scans were initiated at 114 min (IQR 100–121 min) and 226 min (IQR 209–237 min) after the injection, respectively. Among the 23 patients, 14 underwent surgery that included either a biopsy or resection after ^{18}F-FMISO PET, and these 14 patients were pathologically confirmed to have gliomas (n=12), glial proliferation (n=1), or a tumefactive demyelinating lesion (n=1).

The interval between ^{18}F-FMISO PET and the surgical procedure was 8 days (IQR 5–14 days).

Of the remaining 9 patients, 5 did not undergo surgery but were strongly suspected of having recurrent glioma (GBM, n=2; anaplastic oligodendroglioma, n=2; oligodendroglioma, n=1) based on previous pathological diagnoses. One patient was clinically diagnosed as having a tumefactive demyelinating lesion, 2 patients were clinically diagnosed with metastatic brain tumors (origins: breast and renal cancer), and the diagnosis of the remaining patient was unknown because he was transferred to another hospital.

Gray-to-white matter contrast of background brain tissue

In the visual assessment, all 23 cases showed positive GWC at 2 hr, whereas only five patients showed positive GWC (21.7%) at 4 hr ($p<0.0001$).

In our quantitative analysis, the SUVmean in the cerebral gray matter was 1.23 (IQR 1.10–1.32) at 2 hr, and the SUVmean significantly decreased to 1.04 (IQR 0.95–1.16) at 4 hr ($p<0.0001$). The SUVmean values in the cerebral white matter (1.04, IQR 0.95–1.16 *vs.* 1.02, IQR 0.93–1.13, $p=0.01$) and in the cerebellar cortex (1.30, IQR 1.23–1.47 *vs.* 1.17, IQR 1.12–1.35, $p<0.0001$) and the gray-to-white matter ratio (1.17,

IQR 1.14–1.19 *vs.* 1.09, IQR 1.07–1.10, $p<0.0001$) were also significantly decreased from 2 to 4 hr (Fig. 3).

Lesion uptake (all patients)

At 2 hr after the injection of ^{18}F-FMISO, there were 4 lesions with negative uptake and 19 lesions with positive uptake. Between 2 hr and 4 hr, the visual scores were changed in 9 patients (39.1%): 3 patients showed an increase and 6 patients a decrease in the visual scores. In the remaining 14 patients the scores were unchanged. Therefore, 7 and 16 lesions were scored as showing low and high uptake at 4 hr, respectively.

Tumor lesion uptake of histologically confirmed glioma

Histological diagnosis of glioma was made in 7 GBM and 5 non-GBM patients (Table 2). In the visual assessment of images obtained at 2 hr, 6 of the 7 GBM patients showed positive uptake and the remaining patient showed negative uptake. In contrast, at 4 hr, there were 7 patients with positive uptake and no lesion with negative uptake. Regarding the non-GBMs, 5 patients showed positive uptake at 2 hr, and all 5 of these cases showed negative uptake at 4 hr. The sensitivity, specificity, and accuracy for

diagnosing GBMs were 100%, 100%, and 100% for 4 hr, respectively, which were all superior to the corresponding values at 2 hr: 85.8%, 0.0%, and 50.0%.

In our semi-quantitative evaluation, we observed that the SUVmax of the GBMs increased significantly between 2 and 4 hr (2.20, IQR 1.67–3.32 *vs.* 2.65, IQR 1.74–4.41, p=0.016), and the TNR also increased significantly between 2 and 4 hr (1.75, IQR 1.40–2.38 *vs.* 2.35, IQR 1.67–3.60, p=0.016). Note that all of the GBM cases showed increasing SUVmax values. In contrast, the non-GBMs showed no significant difference in either index between 2 and 4 hr (SUVmax: 1.43, IQR 1.30–1.65 *vs.* 1.36, IQR 1.14–1.47, p=0.06; TNR: 1.16, IQR 1.00–1.27 *vs.* 1.06, IQR 0.99–1.30, p=0.31) (Fig. 4).

Through ROC curve analysis using TNR, both GBM and non-GBM were well-differentiated both at 2 hr and 4 hr (Fig. 5). The cut-off values of TNR were 1.35 for 2 hr and 1.51 for 4 hr. Both of area under ROC curves were 1.00.

Discussion

We assessed PET images obtained at 2 and 4 hr after ^{18}F-FMISO injection. In the background brain tissue, the GWC was significantly decreased at 4 hr compared to that observed at 2 hr. Visual scores were changed in 9 patients (39.1%) from 2 hr to 4 hr. From 2 to 4 hr after the ^{18}F-FMISO injection, the non-GBMs showed a trend of change

from tracer-positive to -negative, while the GBMs remained significantly positive for ^{18}F-FMISO

^{18}F-FMISO is the most commonly used PET tracer for detecting hypoxia. Oxygen tension in tumors has been measured in patients by directly inserting polarographic needle electrodes into the tumors [25-27], but this measurement is invasive and less reproducible. As an alternative, ^{18}F-FMISO PET is a promising and noninvasive method for *in vivo* hypoxia imaging [5-8]. Several research groups suggested that ^{18}F-FMISO accumulation may increase sharply under partial pressure of oxygen (pO_2) at 10–20 mmHg [28, 29]. The ^{18}F-FMISO PET identification of hypoxia proceeds through several steps. First, the blood flow distributes ^{18}F-FMISO in the cells by passive diffusion. When oxygen is abundant in normally oxygenated cells, the parent compound is regenerated by reoxidation and washed out from the tissue. In the hypoxic region, the reduced ^{18}F-FMISO is not regenerated by reoxidation, and the remaining ^{18}F-FMISO binds to intracellular peptides or is conjugated to glutathione [30, 31].

Since ^{18}F-FMISO is a lipophilic compound, it takes a longer time (approximately 4 hr) to be excreted from blood and normal tissues compared to the hydrophilic tracers sometimes used to detect hypoxia (approximately 1 hr) [32]. Our present finding of relatively high gray-to-white matter contrast at 2 hr suggests that the influence of the

blood flow remains; in other words, the wash-out is not sufficient for evaluation of a patient's hypoxia status.

In the WHO criteria, “glioblastoma” is defined as having palisading necrosis in addition to anaplasia and mitotic activity [19]. Intra-tumoral necrosis has been thought to cause hypoxia of surrounding tissue [33, 34]. Although glioblastomas exhibit abundant angiogenesis, the blood vessels are structurally and functionally abnormal, leading to ineffective perfusion and thus to tumor hypoxia [35]. Hypoxia not only weakens the DNA-damaging effects of low linear energy transfer radiations (i.e., X-ray and gamma-ray) [36]; it also inhibits the degradation of hypoxia inducible factor (HIF) and thus promotes a number of cell proliferation genes causing chemo-resistance, adaptation to hypoxia, metastasis, and invasion [37]. Sato et al. reported that ^{18}F-FMISO uptake at 4 hr after injection was significantly higher in patients with high expression of Ki-67 and HIF-1α [38]. However, there have been no reports investigating which scan time after injection is most appropriate for the assessment of correlation between ^{18}F-FMISO uptake and these histological parameters. The current standard of treatment for a histologically diagnosed GBM includes resection followed by adjuvant radiation and chemotherapy [39]. However, GBMs typically recur within months, and the median survival from onset is only 15 months [40].

Noninvasive differentiation of GBM and non-GBM is important to avoid insufficient surgery, because the overall survival of patients cannot be prolonged unless the gadolinium-enhanced part of the tumor is completely removed by surgery. The results of our present analyses show that the GBMs were clearly discriminated from the non-GBMs by the ^{18}F-FMISO PET at 4 hr but not by that at 2 hr after the ^{18}F-FMISO injection. We previously showed that ^{18}F-FMISO PET discriminated glioblastoma from less malignant gliomas at 4 hr after ^{18}F-FMISO injection due to the much higher accumulation in GBM *vs.* non-GBM at that time point [21]. However, Cher et al. [12] and Yamamoto et al. [17] demonstrated that grade III gliomas showed elevated ^{18}F-FMISO uptake at 2 hr after injection. This discrepancy is probably due to the difference in the uptake time.

A kinetic analysis of ^{18}F-FMISO uptake indicated the time-dependent uptake characteristics of ^{18}F-FMISO and suggested that a longer uptake time may be more beneficial to evaluate tumor hypoxia. Thorwarth et al. discussed a theoretical problem with the images 2 hr after injection of ^{18}F-FMISO. They reported that hot spots occurred on the ^{18}F-FMISO images after 2 hr but disappeared after 4 hr based on the kinetic analysis of a dynamic ^{18}F-FMISO PET dataset. This result suggested that the high uptake on the images after 2 hr might reflect a high initial influx of the tracer due to

increased blood flow as well as hypoxia [41]. Early reports by Grunbaum et al. also suggested that longer diffusion times might be required to achieve acceptable target/background ratios for hypoxia imaging [42]. Nevertheless, most of the relevant studies adopted 2-hr protocols [8, 9, 12, 13, 15, 17], possibly because a shorter protocol would generally be more acceptable in clinical settings. In the present study, all grades of glioma showed an elevated accumulation of ^{18}F-FMISO at 2 hr after ^{18}F-FMISO injection. Conversely, at 4 hr, all of the non-GBM lesions showed negative ^{18}F-FMISO uptake. This data provides evidence of the uptake time-related differences mentioned above.

In addition, our present findings demonstrated that the 2-hr images showed strong contrast between gray and white matter, and this contrast disappeared at 4 hr. This result also supports the concept that the influence of the blood flow remained at 2 hr. We speculate that the ^{18}F-FMISO was not sufficiently washed out from the normoxic cells at the 2-hr timepoint. Grkovski et al. evaluated the hypoxic condition in detail by using kinetic modeling obtained by dynamic imaging [43]. In their report, a static image of ^{18}F-FMISO PET might lead to a misinterpretation of hypoxic lesions. However, the images obtained at 4 hr may be preferable as a reasonable surrogate, since it is clinically difficult to perform continuous imaging for a long period of time. Static images also

have better image quality than dynamic and parametric images.

Peeters et al. demonstrated that ^{18}F-FMISO uptake was still increasing at 6 hr in their laboratory animal study [44]. However, in a clinical setting, it is difficult to perform a scan at 6 hr post-injection, and the reduced counts may cause a lower signal-to-noise ratio.

Study limitations

This study has some methodological limitations. It was a retrospective analysis of patients at a single center and included a relatively small cohort of subjects (n=23) who underwent ^{18}F-FMISO PET imaging for suspected brain tumors. In this retrospective study, histological measurements of hypoxia, such as HIF-1 immunohistochemical staining, and in-vivo blood flow imaging, such as O-15 water PET, are lacking. Further studies are needed to correlate such information with ^{18}F-FMISO uptake. Nevertheless, these results might have clinical implications for the staging algorithm for patients with a suspected brain tumor.

Conclusion

For the evaluation of hypoxia in brain tumors and especially to distinguish GBMs

from non-GBMs, our current data suggest that ^{18}F-FMISO PET images should be obtained at 4 hr rather than at 2 hr after the ^{18}F-FMISO injection.

Acknowledgments

We thank the staff members of the Department of Nuclear Medicine, the Central Institute of Isotope Science, the Department of Cancer Pathology, Hokkaido University, and the Department of Radiology, Hokkaido University Hospital for their support of this work.

Ethical approval

All procedures involving human participants were in accordance with the ethical standards of the institutional and/or national research committee and with the principles of the 1964 Declaration of Helsinki and its later amendments or comparable ethical standards. A portion of our results were presented at the SNMMI 2018 Conference (J Nucl Med May 1, 2015 vol. 56 no. supplement 3 373).

Conflict of interest

All authors have no conflicts of interest to disclose.

Financial disclosure

This research was supported in part by a Grant-in-Aid for General Scientific Research from the Japan Society for the Promotion of Science (Ko.Ke., 19K17127).

Informed consent

The requirement for written informed consent was waived due to the retrospective nature of this study.

References

1. Hirata K, Yamaguchi S, Shiga T, Kuge Y, Tamaki N. The Roles of Hypoxia Imaging Using (18)F-Fluoromisonidazole Positron Emission Tomography in Glioma Treatment. J Clin Med. 2019;8. doi:10.3390/jcm8081088.

2. Tamaki N, Hirata K. Tumor hypoxia: a new PET imaging biomarker in clinical oncology. Int J Clin Oncol. 2016;21:619-25. doi:10.1007/s10147-015-0920-6.

3. Kobayashi H, Hirata K, Yamaguchi S, Terasaka S, Shiga T, Houkin K. Usefulness of FMISO-PET for glioma analysis. Neurol Med Chir (Tokyo). 2013;53:773-8. doi:10.2176/nmc.ra2013-0256.

4. Janssen HL, Haustermans KM, Balm AJ, Begg AC. Hypoxia in head and neck cancer: how much, how important? Head Neck. 2005;27:622-38. doi:10.1002/hed.20223.

5. Eschmann SM, Paulsen F, Bedeshem C, Machulla HJ, Hehr T, Bamberg M, et al. Hypoxia-imaging with (18)F-Misonidazole and PET: changes of kinetics during radiotherapy of head-and-neck cancer. Radiother Oncol. 2007;83:406-10. doi:10.1016/j.radonc.2007.05.014.

6. Rasey JS, Koh WJ, Evans ML, Peterson LM, Lewellen TK, Graham MM, et al. Quantifying regional hypoxia in human tumors with positron emission tomography of [18F]fluoromisonidazole: a pretherapy study of 37 patients. International journal of radiation oncology, biology, physics. 1996;36:417-28.

7. Koh WJ, Rasey JS, Evans ML, Grierson JR, Lewellen TK, Graham MM, et al. Imaging of hypoxia in human tumors with [F-18]fluoromisonidazole. International journal of radiation oncology, biology, physics. 1992;22:199-212.

8. Rajendran JG, Wilson DC, Conrad EU, Peterson LM, Bruckner JD, Rasey JS, et al. [(18)F]FMISO and [(18)F]FDG PET imaging in soft tissue sarcomas: correlation of hypoxia, metabolism and VEGF expression. Eur J Nucl Med Mol Imaging. 2003;30:695-704. doi:10.1007/s00259-002-1096-7.

9. Valk PE, Mathis CA, Prados MD, Gilbert JC, Budinger TF. Hypoxia in human gliomas: demonstration by PET with fluorine-18-fluoromisonidazole. J Nucl Med. 1992;33:2133-7.

10. Toyonaga T, Yamaguchi S, Hirata K, Kobayashi K, Manabe O, Watanabe S, et al. Hypoxic glucose metabolism in glioblastoma as a potential prognostic factor. Eur J Nucl Med Mol Imaging. 2017;44:611-9. doi:10.1007/s00259-016-3541-z.

11. Bruehlmeier M, Roelcke U, Schubiger PA, Ametamey SM. Assessment of hypoxia and perfusion in human brain tumors using PET with 18F-fluoromisonidazole and 15O-H2O. J Nucl Med. 2004;45:1851-9.

12. Cher LM, Murone C, Lawrentschuk N, Ramdave S, Papenfuss A, Hannah A, et al. Correlation of hypoxic cell fraction and angiogenesis with glucose metabolic rate in gliomas

using 18F-fluoromisonidazole, 18F-FDG PET, and immunohistochemical studies. J Nucl Med. 2006;47:410-8.

13. Spence AM, Muzi M, Swanson KR, O'Sullivan F, Rockhill JK, Rajendran JG, et al. Regional hypoxia in glioblastoma multiforme quantified with [18F]fluoromisonidazole positron emission tomography before radiotherapy: correlation with time to progression and survival. Clin Cancer Res. 2008;14:2623-30. doi:10.1158/1078-0432.ccr-07-4995.

14. Swanson KR, Chakraborty G, Wang CH, Rockne R, Harpold HL, Muzi M, et al. Complementary but distinct roles for MRI and 18F-fluoromisonidazole PET in the assessment of human glioblastomas. J Nucl Med. 2009;50:36-44. doi:10.2967/jnumed.108.055467.

15. Szeto MD, Chakraborty G, Hadley J, Rockne R, Muzi M, Alvord EC, Jr., et al. Quantitative metrics of net proliferation and invasion link biological aggressiveness assessed by MRI with hypoxia assessed by FMISO-PET in newly diagnosed glioblastomas. Cancer Res. 2009;69:4502-9. doi:10.1158/0008-5472.can-08-3884.

16. Kawai N, Maeda Y, Kudomi N, Miyake K, Okada M, Yamamoto Y, et al. Correlation of biological aggressiveness assessed by 11C-methionine PET and hypoxic burden assessed by 18F-fluoromisonidazole PET in newly diagnosed glioblastoma. Eur J Nucl Med Mol Imaging. 2011;38:441-50. doi:10.1007/s00259-010-1645-4.

17. Yamamoto Y, Maeda Y, Kawai N, Kudomi N, Aga F, Ono Y, et al. Hypoxia assessed by 18F-fluoromisonidazole positron emission tomography in newly diagnosed gliomas. Nucl Med Commun. 2012;33:621-5. doi:10.1097/MNM.0b013e3283529984.

18. Yamaguchi S, Hirata K, Toyonaga T, Kobayashi K, Ishi Y, Motegi H, et al. Change in 18F-Fluoromisonidazole PET Is an Early Predictor of the Prognosis in the Patients with Recurrent High-Grade Glioma Receiving Bevacizumab Treatment. PLoS One. 2016;11:e0167917. doi:10.1371/journal.pone.0167917.

19. Louis DN, Ohgaki H, Wiestler OD, Cavenee WK, Burger PC, Jouvet A, et al. The 2007 WHO classification of tumours of the central nervous system. Acta Neuropathol. 2007;114:97-109. doi:10.1007/s00401-007-0243-4.

20. Louis DN, Perry A, Reifenberger G, von Deimling A, Figarella-Branger D, Cavenee WK, et al. The 2016 World Health Organization Classification of Tumors of the Central Nervous System: a summary. Acta Neuropathol. 2016;131:803-20. doi:10.1007/s00401-016-1545-1.

21. Hirata K, Terasaka S, Shiga T, Hattori N, Magota K, Kobayashi H, et al. (1)(8)F-Fluoromisonidazole positron emission tomography may differentiate glioblastoma multiforme from less malignant gliomas. Eur J Nucl Med Mol Imaging. 2012;39:760-70. doi:10.1007/s00259-011-2037-0.

22. Toyonaga T, Hirata K, Yamaguchi S, Hatanaka KC, Yuzawa S, Manabe O, et al.

F-fluoromisonidazole positron emission tomography can predict pathological necrosis of brain tumors. Eur J Nucl Med Mol Imaging. 2016. doi:10.1007/s00259-016-3320-x.

23. Kanoto M, Kirii K, Hiraka T, Toyoguchi Y, Sugai Y, Matsuda K, et al. Correlation between hypoxic area in primary brain tumors and WHO grade: differentiation from malignancy using 18F-fluoromisonidazole positron emission tomography. Acta Radiol. 2018;59:229-35. doi:10.1177/0284185117711474.

24. Kobayashi K, Hirata K, Yamaguchi S, Manabe O, Terasaka S, Kobayashi H, et al. Prognostic value of volume-based measurements on (11)C-methionine PET in glioma patients. Eur J Nucl Med Mol Imaging. 2015;42:1071-80. doi:10.1007/s00259-015-3046-1.

25. Evans SM, Judy KD, Dunphy I, Jenkins WT, Hwang WT, Nelson PT, et al. Hypoxia is important in the biology and aggression of human glial brain tumors. Clin Cancer Res. 2004;10:8177-84. doi:10.1158/1078-0432.ccr-04-1081.

26. Lally BE, Rockwell S, Fischer DB, Collingridge DR, Piepmeier JM, Knisely JP. The interactions of polarographic measurements of oxygen tension and histological grade in human glioma. Cancer J. 2006;12:461-6.

27. Collingridge DR, Piepmeier JM, Rockwell S, Knisely JP. Polarographic measurements of oxygen tension in human glioma and surrounding peritumoural brain tissue. Radiother Oncol. 1999;53:127-31.

28. Rasey JS, Nelson NJ, Chin L, Evans ML, Grunbaum Z. Characteristics of the binding of labeled fluoromisonidazole in cells in vitro. Radiat Res. 1990;122:301-8.

29. Kavanagh MC, Sun A, Hu Q, Hill RP. Comparing techniques of measuring tumor hypoxia in different murine tumors: Eppendorf pO2 Histograph, [3H]misonidazole binding and paired survival assay. Radiat Res. 1996;145:491-500.

30. Lee ST, Scott AM. Hypoxia positron emission tomography imaging with 18f-fluoromisonidazole. Semin Nucl Med. 2007;37:451-61. doi:10.1053/j.semnuclmed.2007.07.001.

31. Masaki Y, Shimizu Y, Yoshioka T, Tanaka Y, Nishijima K, Zhao S, et al. The accumulation mechanism of the hypoxia imaging probe "FMISO" by imaging mass spectrometry: possible involvement of low-molecular metabolites. Sci Rep. 2015;5:16802. doi:10.1038/srep16802.

32. Watanabe S, Shiga T, Hirata K, Magota K, Okamoto S, Toyonaga T, et al. Biodistribution and radiation dosimetry of the novel hypoxia PET probe [(18)F]DiFA and comparison with [(18)F]FMISO. EJNMMI Res. 2019;9:60. doi:10.1186/s13550-019-0525-6.

33. Oliver L, Olivier C, Marhuenda FB, Campone M, Vallette FM. Hypoxia and the malignant glioma microenvironment: regulation and implications for therapy. Curr Mol Pharmacol. 2009;2:263-84.

34. Flynn JR, Wang L, Gillespie DL, Stoddard GJ, Reid JK, Owens J, et al.

Hypoxia-regulated protein expression, patient characteristics, and preoperative imaging as predictors of survival in adults with glioblastoma multiforme. Cancer. 2008;113:1032-42. doi:10.1002/cncr.23678.

35. Bekaert L, Valable S, Lechapt-Zalcman E, Ponte K, Collet S, Constans JM, et al. [18F]-FMISO PET study of hypoxia in gliomas before surgery: correlation with molecular markers of hypoxia and angiogenesis. Eur J Nucl Med Mol Imaging. 2017;44:1383-92. doi:10.1007/s00259-017-3677-5.

36. Gray LH, Conger AD, Ebert M, Hornsey S, Scott OC. The concentration of oxygen dissolved in tissues at the time of irradiation as a factor in radiotherapy. Br J Radiol. 1953;26:638-48. doi:10.1259/0007-1285-26-312-638.

37. Ji Z, Long H, Hu Y, Qiu X, Chen X, Li Z, et al. Expression of MDR1, HIF-1alpha and MRP1 in sacral chordoma and chordoma cell line CM-319. J Exp Clin Cancer Res. 2010;29:158. doi:10.1186/1756-9966-29-158.

38. Sato J, Kitagawa Y, Watanabe S, Asaka T, Ohga N, Hirata K, et al. (18)F-Fluoromisonidazole positron emission tomography (FMISO-PET) may reflect hypoxia and cell proliferation activity in oral squamous cell carcinoma. Oral Surg Oral Med Oral Pathol Oral Radiol. 2017;124:261-70. doi:10.1016/j.oooo.2017.05.506.

39. Stupp R, Brada M, van den Bent MJ, Tonn JC, Pentheroudakis G. High-grade glioma: ESMO Clinical Practice Guidelines for diagnosis, treatment and follow-up. Ann Oncol. 2014;25 Suppl 3:iii93-101. doi:10.1093/annonc/mdu050.

40. Thakkar JP, Dolecek TA, Horbinski C, Ostrom QT, Lightner DD, Barnholtz-Sloan JS, et al. Epidemiologic and molecular prognostic review of glioblastoma. Cancer Epidemiol Biomarkers Prev. 2014;23:1985-96. doi:10.1158/1055-9965.EPI-14-0275.

41. Thorwarth D, Eschmann SM, Paulsen F, Alber M. A kinetic model for dynamic [18F]-Fmiso PET data to analyse tumour hypoxia. Phys Med Biol. 2005;50:2209-24. doi:10.1088/0031-9155/50/10/002.

42. Grunbaum Z, Freauff SJ, Krohn KA, Wilbur DS, Magee S, Rasey JS. Synthesis and characterization of congeners of misonidazole for imaging hypoxia. J Nucl Med. 1987;28:68-75.

43. Grkovski M, Emmas SA, Carlin SD. (18)F-Fluoromisonidazole Kinetic Modeling for Characterization of Tumor Perfusion and Hypoxia in Response to Antiangiogenic Therapy. J Nucl Med. 2017;58:1567-73. doi:10.2967/jnumed.117.190892.

44. Peeters SG, Zegers CM, Lieuwes NG, van Elmpt W, Eriksson J, van Dongen GA, et al. A comparative study of the hypoxia PET tracers [(1)(8)F]HX4, [(1)(8)F]FAZA, and [(1)(8)F]FMISO in a preclinical tumor model. International journal of radiation oncology, biology, physics. 2015;91:351-9. doi:10.1016/j.ijrobp.2014.09.045.

Table 1. Patient characteristics

Age, yrs	61 (47-68)
Male, n	10
Injection dose, MBq	395 (388-410)
Duration from injection and first scan, min	114 (100-121)
Duration from injection and second scan, min	226 (209-237)
Histologically diagnosed glioma patients (n=12):	
GBM	7
Non-GBM	5
Recurrent glioma from GBM	2
Recurrent glioma from AO	3
Metastasis	2
Tumefactive demyelinating	2
Glial proliferation	1
Unknown	1

Data are represented as the median (interquartile range) or number.

GBM, glioblastoma; AO, anaplastic oligodendroglioma.

Table 2. Characteristics of the 12 patients with histologically diagnosed glioma

Patient	Gender	Diag.	WHO grade	SUVmax 2 hr	SUVmax 4 hr	TNR 2 hr	TNR 4 hr	Visual score 2 hr	Visual score 4 hr
1	M	OD	II	1.70	1.47	1.16	1.06	pos.	neg.
2	M	OD	II	1.25	1.19	1.00	1.03	pos.	neg.
3	M	GBM	IV	1.66	1.74	1.40	1.67	neg.	pos.
4	M	GBM	IV	3.32	4.41	2.38	3.76	pos.	pos.
5	F	GBM	IV	3.55	4.65	2.39	3.60	pos.	pos.
6	F	AA	III	1.39	1.14	0.99	0.90	pos.	neg.
7	M	AO	III	1.43	1.12	1.20	0.99	pos.	neg.
8	M	GBM	IV	2.85	3.89	2.11	3.34	pos.	pos.
9	M	GBM	IV	1.67	1.67	1.35	1.51	pos.	pos.
10	F	GBM	IV	2.20	2.65	1.70	2.22	pos.	pos.
11	M	GBM	IV	1.92	2.57	1.75	2.35	pos.	pos.
12	F	DA	II	1.55	1.36	1.27	1.29	pos.	neg.

AA: anaplastic astrocytoma; AO: anaplastic oligodendroglioma; DA: diffuse astrocytoma; GBM: glioblastoma; neg.: negative; OD: oligodendroglioma; pos.: positive; SUVmax: maximum standardized uptake value; TNR: tumor-to-normal ratio; WHO: World Health Organization.

Figure legends

Fig. 1. Study protocol. PET images were acquired twice, at 2 and 4 hr after a single ^{18}F-FMISO injection.

Fig. 2. Representative cases of glioblastoma (A) and grade III glioma (B). **A:** The ^{18}F-FMISO uptake of the tumor at the left parietal lobe was classified as negative at 2 hr but positive at 4 hr. At 2 and 4 hr, the SUVmax values were 1.66 and 1.74 and the TNR values were 1.40 and 1.67, respectively. The gray-to-white matter contrast (GWC) in the background brain tissue was positive at 2 hr but negative at 4 hr. **B:** At 2 and 4 hr, the ^{18}F-FMISO uptake of the tumor at the right temporal lobe was classified as positive and negative, respectively; the SUVmax values were 1.43 and 1.12, and the TNRs were 1.20 and 0.99. The GWC was positive at 2 hr but negative at 4 hr.

Fig. 3. Quantitative results of normal brain tissues. The SUVmean values of cerebral gray matter (**A**), cerebral white matter (**B**), cerebellar cortex (**C**), and gray-to-white matter ratio (**D**) were significantly decreased at 4 hr compared to 2 hr.

Fig. 4. The difference in the tracer uptake between 2 and 4 hr. The SUVmax of a

non-GBM tumor (**A**), the SUVmax of a GBM (**B**), the TNR of a non-GBM (**C**), and the TNR of a GBM (**D**) were compared between 2 and 4 hr. There were no significant differences in the non-GBM, but in the GBM, both the SUVmax and the TNR increased significantly from 2 to 4 hr. GBM, glioblastoma; SUVmax, maximum standardized uptake value; TNR, tumor-to-normal ratio.

Fig 5. ROC curves for diagnosis of GBM and non-GBM by tumor TNR.

TNR at 2hr (A) and at 4 hr (B) were compared between non-GBM. ROC curve using TNR showed that both GBM and non-GBM were well-differentiated both at 2 hr (C) and 4 hr (D).

ROC, receiver operating characteristic; GBM, glioblastoma; TNR, tumor-to-normal ratio; AUC, area under the curve.

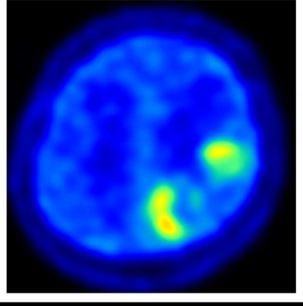

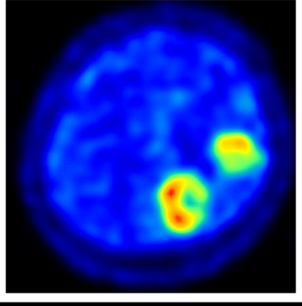

0

2

4

hr

^{18}F-FMISO
i.v.

1st scan

2nd scan

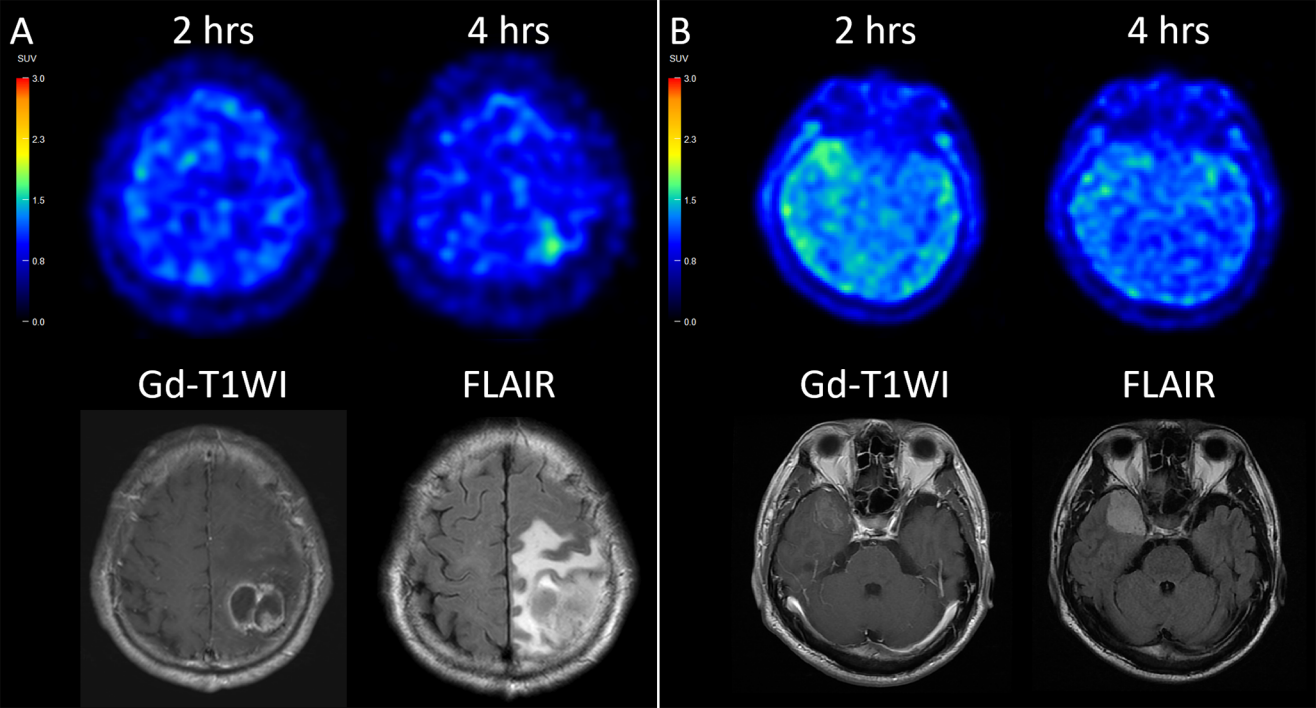
A
2 hrs
4 hrs
SUV
3.0
2.3
1.5
0.8
0.0
Gd-T1WI
FLAIR
B
2 hrs
4 hrs
SUV
3.0
2.3
1.5
0.8
0.0
Gd-T1WI
FLAIR

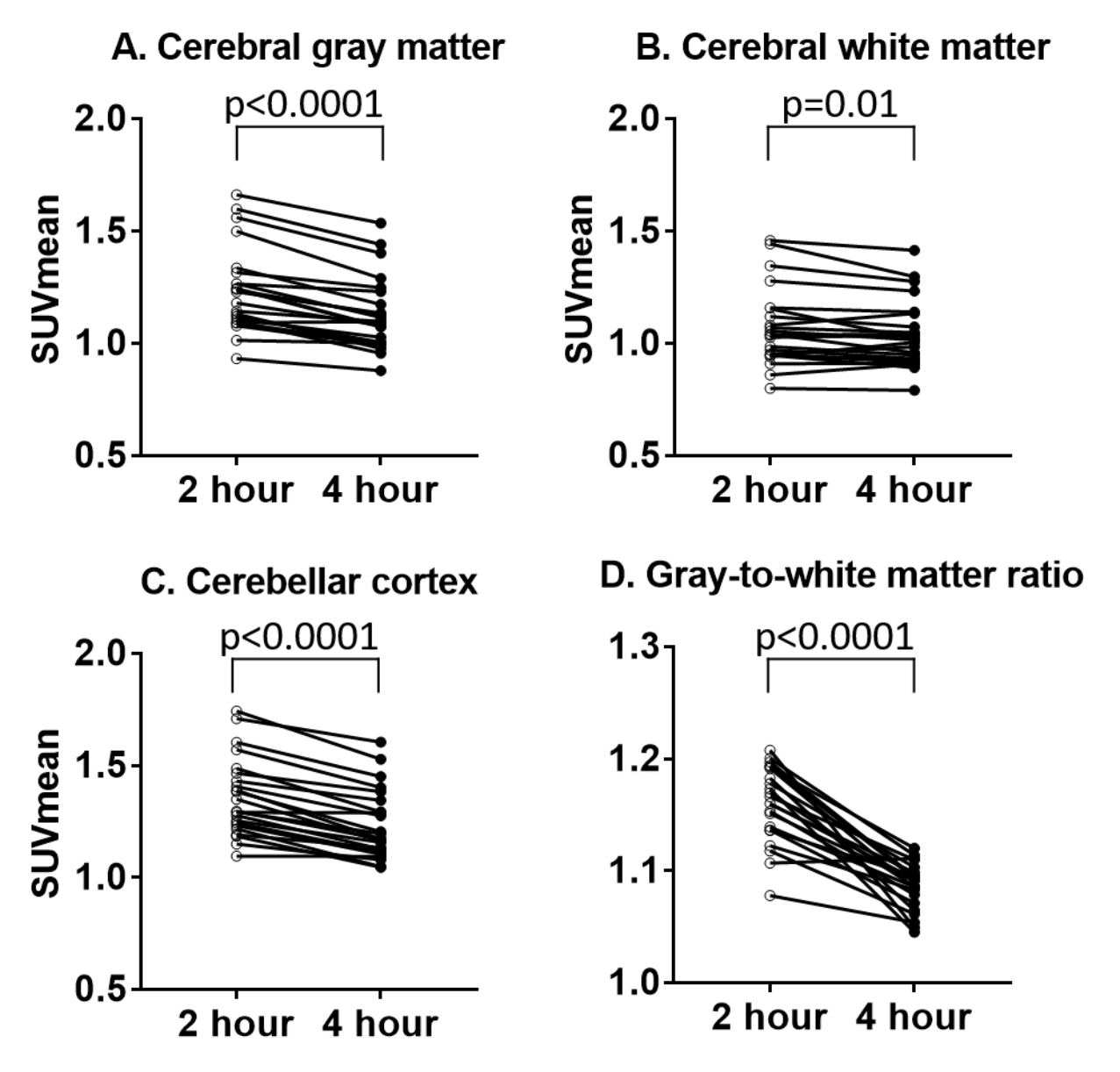
A. Cerebral gray matter
p<0.0001
SUVmean
2.0
1.5
1.0
0.5
2 hour
4 hour
B. Cerebral white matter
p=0.01
SUVmean
2.0
1.5
1.0
0.5
2 hour
4 hour
C. Cerebellar cortex
p<0.0001
SUVmean
2.0
1.5
1.0
0.5
2 hour
4 hour
D. Gray-to-white matter ratio
p<0.0001
1.3
1.2
1.1
1.0
2 hour
4 hour

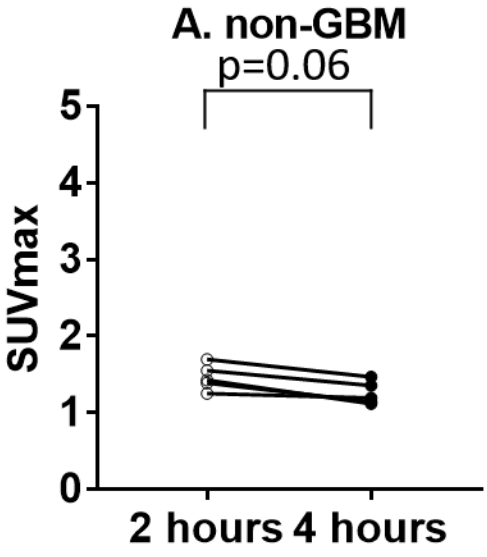
A. non-GBM
p=0.06
SUVmax
5
4
3
2
1
0
2 hours 4 hours

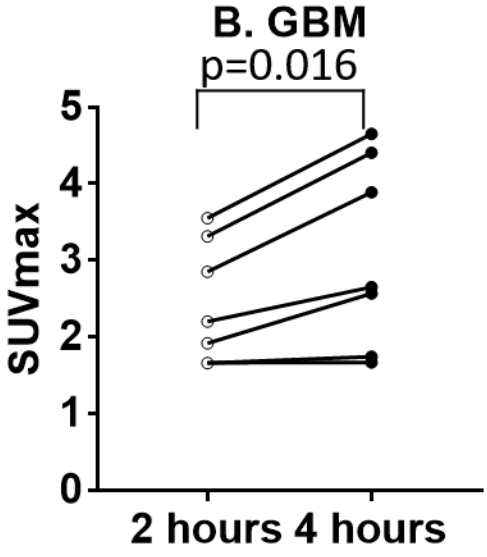
B. GBM
p=0.016
SUVmax
5
4
3
2
1
0
2 hours 4 hours

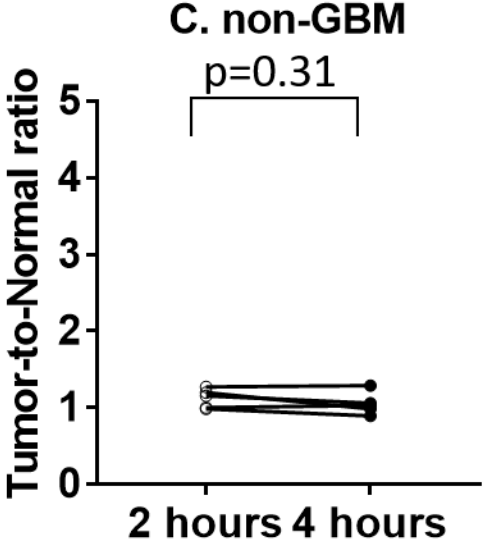
C. non-GBM
p=0.31
Tumor-to-Normal ratio
5
4
3
2
1
0
2 hours 4 hours

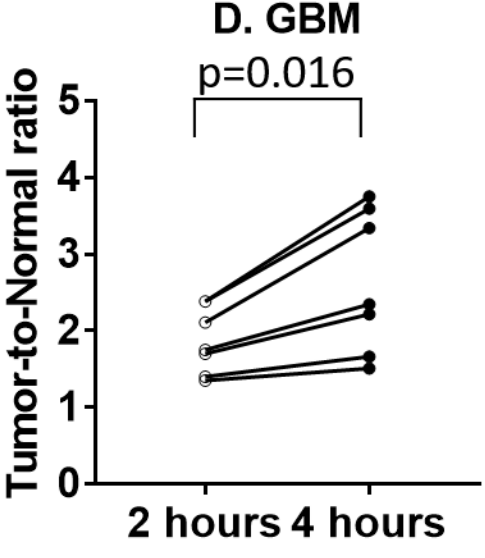
D. GBM
p=0.016
Tumor-to-Normal ratio
5
4
3
2
1
0
2 hours 4 hours

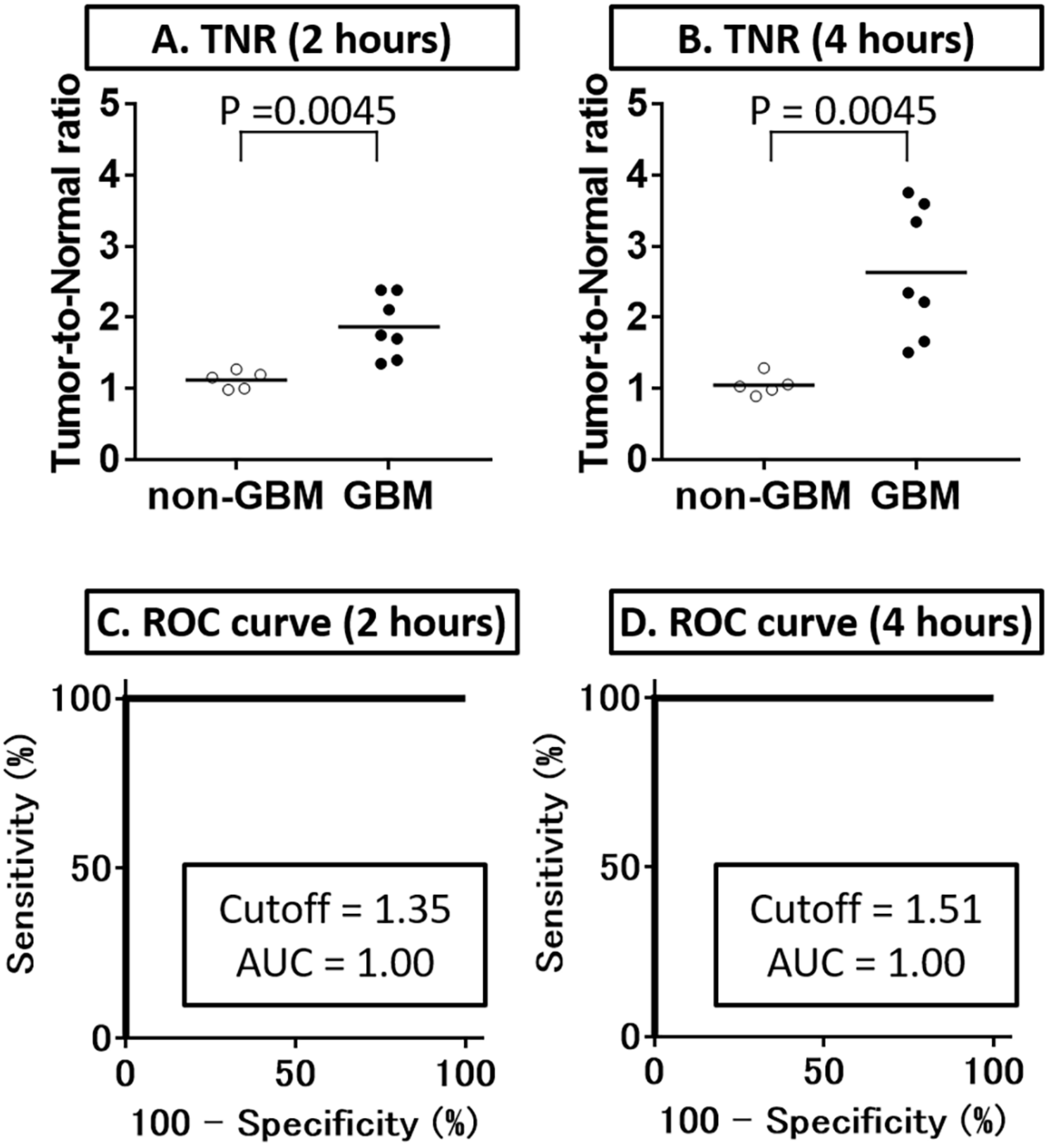
A. TNR (2 hours)
Tumor-to-Normal ratio
P =0.0045
non-GBM
GBM
B. TNR (4 hours)
Tumor-to-Normal ratio
P = 0.0045
non-GBM
GBM
C. ROC curve (2 hours)
Sensitivity (%)
Cutoff = 1.35
AUC = 1.00
100 − Specificity (%)
D. ROC curve (4 hours)
Sensitivity (%)
Cutoff = 1.51
AUC = 1.00
100 − Specificity (%)